



OPEN

On geometry parameterization for simulation-driven design closure of antenna structures

Slawomir Koziel^{1,2} & Anna Pietrenko-Dabrowska²✉

Full-wave electromagnetic (EM) simulation tools have become ubiquitous in antenna design, especially final tuning of geometry parameters. From the reliability standpoint, the recommended realization of EM-driven design is through rigorous numerical optimization. It is a challenging endeavor with the major issues related to the high computational cost of the process, but also the necessity of handling several objectives and constraints over often highly-dimensional parameter spaces. From the numerical perspective, making decisions about the formulation of the optimization problem, the approach to handling the design constraints, but also parameterization of the antenna geometry, are all non-trivial. At the same time, these issues are interleaved, and may play an important role in the performance and reliability of the simulation-based design closure process. This paper demonstrates that the approach to arranging the structure parameterization (e.g., the use of absolute or relative parameters) may have a major effect of the optimization outcome. Our investigations are carried out using three broadband monopole antennas optimized under different scenarios and using different parameterizations. In particular, the results indicate that relative parameterization is preferred for optimization of input characteristics, whereas absolute parameterization is more suitable for size reduction.

The last decade or so has witnessed a significant increase in the complexity of antenna geometries^{1–5}. This can be mainly attributed to the emergence of new technologies (4G and 5G wireless communications⁶, medical imaging⁷, wireless sensing⁸, implantable devices⁹), but also trends towards miniaturization and portability (mobile communications¹⁰, internet of things, IoT¹¹, wearable devices¹²). On the one hand, to fulfil the performance requirements imposed by the needs pertinent to specific application areas, antenna structures have to implement additional functionalities (multi-band operation¹³, tunability¹⁴, circular polarization¹⁵), but also offer improved characteristics (high gain¹⁶, broadband operation¹⁷, high element isolation in MIMO systems¹⁸, etc.). This requires incorporation of a variety of geometrical alterations (stubs¹⁹, slots²⁰, defected ground structures²¹, metamaterial-based components²²), which makes the designs increasingly sophisticated and described by large numbers of parameters. Also, the use of full-wave electromagnetic (EM) simulation tools is instrumental in ensuring evaluation reliability. On the other hand, miniaturization trends lead to additional challenges as size reduction is detrimental to antenna electrical properties^{23,24}. In any case, EM-driven design becomes a matter of practical necessity in general, whereas simulation-based parameter tuning belongs to the most important stages of the antenna design cycle.

EM-simulation-based parameter tuning of antenna systems is imperative, yet it is a daunting task. Its fundamental bottlenecks include high computational cost, a typically large number of parameters, but also the necessity of handling several objectives and constraints. Over the years, the literature offered a variety of algorithmic solutions that aim at alleviating these difficulties. Some of available options include methods for expediting the EM-driven optimization procedures, e.g., adjoint sensitivities²⁵, sparse Jacobian updates²⁶, surrogate-assisted methods, involving both data-driven (kriging²⁷, radial-basis functions²⁸, neural networks²⁹, Gaussian process regression³⁰, ensemble learning methods³¹), and physics-based models (space mapping³², manifold mapping³³, response correction methods^{34,35}, cognition-driven design³⁶), or machine learning techniques^{37,38}. Handling of multiple objectives is often realized using surrogate-enhanced population-based methods^{39–41} or penalty function approaches (e.g., for size reduction under multiple constraints imposed on antenna electrical performance⁴²), whereas dimensionality issues are often addressed using high-dimensional model representation (HDMR)⁴³, principal component analysis (PCA)⁴⁴, model order reduction methods⁴⁵, or—in the context of response surface

¹Engineering Optimization and Modeling Center, Reykjavik University, 102 Reykjavik, Iceland. ²Faculty of Electronics, Telecommunications and Informatics, Gdansk University of Technology, 80-233 Gdańsk, Poland. ✉email: anna.dabrowska@pg.edu.pl

approximation—techniques such as orthogonal matching pursuit (OMP)⁴⁶, or least angle regression (LAR)⁴⁷. Surrogate-based methods are also popular for aiding global optimization^{48,49}. The improvement of local search reliability (e.g., under the lack of quality initial designs) can be achieved using feature-based optimization (FBO)-type of approaches^{50,51}. Accelerating specific simulation-driven design tasks can be realized using particular classes of replacement models (e.g., polynomial chaos expansion, PCE, for uncertainty quantification^{52,53}).

One of the important aspects of antenna optimization in general, and EM-driven design in particular, is appropriate geometry parameterization of the structure under design. As a matter of fact, this aspect is almost never explicitly discussed in the literature, although parameterization may have some serious implications for the design process reliability. In the vast majority of cases, a natural (or absolute) parameterization is employed, where specific dimensions of the antenna components (radiator width and length, stub lengths, slot distance, ground plane length, etc.) are described using respective variables, typically sized in millimeters. From the perspective of numerical optimization, the fundamental problem incurred by such an approach are design constraints that have to be imposed in order to ensure geometrical consistency of the structure, e.g., to have the radiator allocated within the dielectric substrate outline, the ground-plane slots contained within the ground plane rather than cutting it into disjoint patches, etc. Most of these constraints are linear, although nonlinear ones may also be necessary, e.g., to ensure that certain components are allocated in the interior of circular-shaped slots, etc. The presence of constraints makes the optimization problem more challenging, which is of particular importance when handling EM-simulated antenna responses. The latter is due to the numerical noise inherent to simulated characteristics of the device. A less popular alternative is relative parameterization, where the antenna components are sized in relation to the dimensions of the components encapsulating them (e.g., a radiator slot length being a fraction the radiator size, or substrate size being a sum of encapsulated components such as the feed line length, radiator length, etc.). A clear advantage is that the number of geometrical constraints can be reduced to a minimum (often to zero), which leads to an interval-based parameter space, significantly easier to handle.

This paper investigates the importance of geometry parameterization from the perspective of EM-driven tuning of antenna structures. Two types of parameterization are juxtaposed, referred to the absolute and the relative ones (as outlined in the previous paragraph), along with their potential advantages and drawbacks from the point of view of solving antenna optimization tasks. Using several exemplary structures of broadband antennas, it is demonstrated that relative parameterization is more suitable for improving electrical properties (primarily, the input characteristics). On the other hand, the absolute parameterization is more beneficial for explicit size reduction, which is a constrained task by itself due to the necessity of maintaining specific acceptance levels for input matching, and, perhaps, other antenna responses. Consistency of the results throughout the benchmark set as well as considerable differences in the optimization process performance, provide conclusive evidence about the importance of the appropriate choice of antenna parameterization within a given EM-based design context.

The originality and the technical contributions of this work can be summarized as follows: (1) formal introduction of absolute and relative antenna parameterizations, (2) qualitative comparison of the benefits and limitations of the absolute and relative parameterizations in the context of different EM-driven design scenarios, (3) comprehensive (based on three antenna structures and multiple optimization runs) and conclusive assessment of the advantages of relative parameterization for matching improvement tasks, and absolute one for size reduction purposes. According to the authors' knowledge, this is the first treatment of this subject (both qualitative and quantitative) in the antenna design optimization literature.

Simulation-driven design of antenna structures: geometry parameterization. This section formally introduces the two types of antenna geometry parameterizations considered in this paper, and discusses their qualitative advantages and disadvantages from the point of view of solving EM-driven design tasks. Quantitative evaluation, based on three antenna structures and two specific design scenarios (size reduction and matching improvement), will be provided in “Results”.

Antenna parameter tuning: problem formulation. The computational model of the antenna structure under design will be denoted as R , where $\mathbf{x} = [x_1 \dots x_n]^T$ is the vector of (independent) adjustable parameters. R is assumed to be evaluated using full-wave EM analysis. $R(\mathbf{x})$ will represent all relevant antenna characteristics at the design \mathbf{x} , in particular, the reflection response $S_{11}(\mathbf{x}, f)$, gain $G(\mathbf{x}, f)$, axial ratio $AR(\mathbf{x}, f)$, etc., for frequencies f within the simulation range of interest. Furthermore, we will denote the antenna size as $A(\mathbf{x})$ (e.g., the footprint area in the case of planar antennas).

The parameter tuning task is formulated as a minimization problem

$$\mathbf{x}^* = \arg \min_{\mathbf{x} \in X} U(\mathbf{x}) \quad (1)$$

where X is the problem domain, discussed at length in “Geometry parameterization: Absolute vs. relative”. In some cases, additional constraints are imposed, which are typically of an inequality type, i.e., $g_k(\mathbf{x}) \leq 0, k = 1, \dots, n_g$.

The objective function is a metric of the design quality, and, therefore, it is problem dependent. Consider the following examples:

- Matching improvement in a specified frequency range F : $U(\mathbf{x}) = \max\{f \in F : |S_{11}(\mathbf{x}, f)|\}$;
- Axial ratio improvement in a specified frequency range F : $U(\mathbf{x}) = \max\{f \in F : AR(\mathbf{x}, f)\}$;
- Size reduction of a planar antenna: $U(\mathbf{x}) = A(\mathbf{x})$

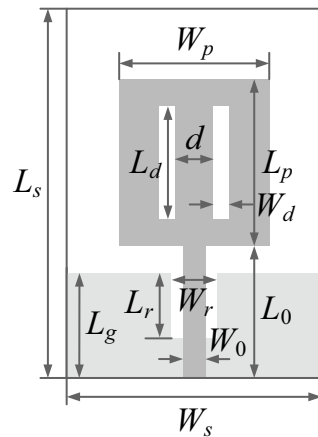


Figure 1. Absolute parameterization for an exemplary monopole antenna⁵⁵ (ground plane marked using the light-shade grey). The geometry is described by the variable vector $\mathbf{x} = [L_s L_0 L_p L_d L_r L_g W_s W_r W_p W_d d]^T$; variable W_0 is normally fixed and adjusted for a given substrate to ensure 50- Ω line impedance. (Microsoft Visio 2016, <https://www.microsoft.com/pl-pl/microsoft-365/visio/>).

Design constraints are often related to antenna geometry itself (cf. “Geometry parameterization: Absolute vs. relative”) but also its electrical and field performance figures. Some common examples include:

- Ensuring that antenna reflection does not exceed -10 dB within the frequency range of interest F : $S(\mathbf{x}) \leq -10$ dB, where $S(\mathbf{x}) = \max\{f \in F: |S_{11}(\mathbf{x}, f)|\}$;
- Ensuring that axial ratio does not exceed 3 dB within the frequency range of interest F : $A_R(\mathbf{x}) \leq 3$ dB, where $A_R(\mathbf{x}) = \max\{f \in F: AR(\mathbf{x}, f)\}$.

As the constraints are often expensive to evaluate (i.e., require EM simulation of the antenna structure), their handling is more convenient when using a penalty function approach⁵⁴. This leads to a problem reformulation, so that we have

$$\mathbf{x}^* = \arg \min_{\mathbf{x}} U_P(\mathbf{x}) \quad (2)$$

where the objective function U_P is defined as

$$U_P(\mathbf{x}) = U(\mathbf{x}) + \sum_{k=1}^{n_g} \beta_k c_k(\mathbf{x}) \quad (3)$$

The second term in (3) is a linear combination of the penalty functions $c_k(\mathbf{x})$ quantifying violations of the respective constraints; β_k are the proportionality (penalty) coefficients. In order to make the objective function setup less dependent on a constraint type and typical tolerance levels, penalty functions may be defined based on relative violations, e.g., for the constraint $S(\mathbf{x}) \leq -10$ dB, one may define $c(\mathbf{x}) = [(S(\mathbf{x}) + 10)/10]^2$.

Geometry parameterization: absolute versus relative. The problem of antenna parameterization is rarely elaborated on in the literature. As a matter of fact, it is one of those aspects of the design process that are usually considered unimportant or straightforward to handle. In practice, it is normally reduced to selecting the crucial dimensions (usually, by means of initial parametric studies), and labelling them accordingly for further processing. The purpose of this work is to indicate the relevance of appropriate handling of antenna parameterization as well as far reaching consequences of inappropriate parameter space definition.

We start by describing the two types of antenna parameterization, referred to as absolute and relative. The absolute parameterization corresponds to what is normally considered in practical antenna design, and, therefore, can also be named a natural one. According to this method, all relevant antenna parameters are simply assigned the labels, and processed (e.g., by the optimization procedures) using absolute dimensions expressed in appropriate units (e.g., millimetres).

Figure 1 shows an example of a monopole antenna with radiator slots and a ground plane slot with all its dimensions labelled accordingly. In this case, the absolute parameterization is in one-to-one correspondence with these labels. Typically, all parameters have assigned their lower and upper bounds, which define the parameter space X . However, in order to maintain the geometrical consistency of the structure one has to impose additional constraints. For example, we have to introduce $L_d < L_p$ (i.e., the radiator slots are contained within the radiator), $L_r < L_g$ (the ground plane slot does not split the ground plane into disjoint parts), or $L_0 + L_p \leq L_s$ (the radiator is contained within the substrate). The full list of the necessary constraints can be found in Table 1. For the antenna of Fig. 1, we have six linear constraints in total, which makes the optimization task more challenging when using this parameterization. These have to be considered in addition to the constraints imposed on antenna characteristics (cf. “Antenna parameter tuning. Problem formulation”).

Characteristic	Parameterization	
	Absolute	Relative
Independent parameters	$\mathbf{x} = [L_s, L_0, L_p, L_d, L_r, L_g, W_s, W_r, W_p, W_d, d]^T$	$\mathbf{x} = [L_s, L_{0r}, L_{pr}, L_{dr}, L_{rr}, L_{gr}, W_s, W_r, W_{pr}, W_d, d_r]^T$
Box constraints	$L_{s,\min} \leq L_s \leq L_{s,\max}; L_{0,\min} \leq L_0 \leq L_{0,\max};$ $L_{p,\min} \leq L_p \leq L_{p,\max}; \dots$ $W_{d,\min} \leq W_d \leq W_{d,\max}; d_{\min} \leq d \leq d_{\max}$	$L_{s,\min} \leq L_s \leq L_{s,\max}; W_{s,\min} \leq W_s \leq W_{s,\max};$ $0 \leq L_{0r}, L_{pr}, L_{dr}, L_{rr}, L_{gr} \leq 1;$ $0 \leq W_{rr}, W_{pr}, d_r \leq 1; W_{d,\min} \leq W_d \leq W_{d,\max}$
Parameter space X	$[L_{s,\min}, L_{s,\max}] \times [L_{0,\min}, L_{0,\max}] \times \dots \times [W_{d,\min}, W_{d,\max}] \times [d_{\min}, d_{\max}]$	$[L_{s,\min}, L_{s,\max}] \times [0, 1] \times \dots \times [0, 1] \times [W_{s,\min}, W_{s,\max}] \times [0, 1] \times [0, 1] \times [0, 1] \times [W_{d,\min}, W_{d,\max}] \times [0, 1]$
Additional constraints	$L_d \leq L_p; d + 2W_d \leq W_p; L_0 + L_p \leq L_s;$ $L_g \leq L_s; W_r \leq W_s; W_p \leq W_s$	None
Additional relationships	None	$L_0 = L_s L_{0r}; L_p = (L_s - L_0) L_{pr}; L_d = L_p L_{dr};$ $L_r = L_g L_{rr}; L_g = L_s L_{gr}; W_r = W_s W_{rr};$ $W_p = W_s W_{pr}; d = (W_p - 2W_d) d_r$

Table 1. Absolute versus relative parameterization for the monopole antenna of Fig. 1.

Feature	Parameterization	
	Absolute	Relative
Parameter space and geometry constraints	Box constraints and (usually) linear constraints on antenna dimensions	Only lower and upper parameter bounds (box constraints)
Handling antenna dimensions	Direct: one-to-one correspondence between parameters and antenna dimensions	Indirect: some dimensions calculated using relative and absolute parameters
Solving optimization tasks		
Pros	Direct account for antenna dimensions (suitable for size reduction tasks)	Reduced number of geometry constraints
Cons	Potentially complex geometry of a feasible region (may lead to additional challenges when handling electrical and field characteristics)	Indirect relationship between design variables and antenna geometry (may not be suitable for size reduction tasks)

Table 2. Absolute versus relative parameterization: Basic properties.

Relative parameterization can be introduced to reduce the number of additional geometry constraints. According to it, most of the parameters are used to dimension particular antenna components in relation to the containing elements (e.g., the radiator slot length with respect to the radiator length, etc.). Only the outer dimensions of the antenna as well as parameters that are inherently small (e.g., slot widths) are treated as absolute. Table 1 contains a full description of this parameterization. It can be noted that a certain number of additional relationships is required (to evaluate the absolute antenna dimensions), but no additional constraints are necessary.

In other words, the parameter space is an interval, which is much easier to handle by local search procedures, let alone nature-inspired algorithms (where constrained optimization is a non-trivial task^{56–58}).

It should be noticed that relative parameterization can be also arranged by introducing alternative absolute parameters such as d_l or d_w so that we have $L_s = L_0 + L_p + d_l$ and $W_s = W_p + 2d_w$, in which case the parameters L_0 , L_p , and W_p can be kept absolute, while retaining the overall advantages of the relative parameterization, i.e., the lack of additional constraints, and the parameter space being the interval.

Qualitative comparison of antenna parameterizations. This section discusses some of the basic properties of the two types of antenna parameterization considered in “Geometry parameterization: Absolute vs. relative”, along with potential implication for solving antenna optimization tasks. These are gathered in Table 2. Perhaps the biggest advantage of relative parameterization is the simplicity of the parameter space, which is an interval. Normally, no additional geometry constraints are necessary, which simplifies handling of the parameters, and increases the range of optimization algorithms that can be employed. On the other hand, absolute parameterization is simpler in terms of providing a direct account for antenna dimensions (one-to-one correspondence between design variables and antenna dimensions). It seems that this might be beneficial for solving tasks such as explicit miniaturization, where antenna dimensions directly contribute to the definition of the objective function. At the same time, this might cause problems when handling objectives related to electrical characteristics, e.g., matching improvement, bandwidth enhancement, gain maximization, axial ratio minimization, etc. It should also be emphasized that the aforementioned potential problems are mainly a result of handling EM-simulated antenna responses, which contain a certain level of numerical noise⁵⁹. The differences between the two parameterizations would most likely not be noticeable if inherently smooth objective functions and constraints were to be processed.

Absolute versus relative parameterization: comparative study. The purpose of this section is a comparative study concerning utilization of the two types of geometry parameterization, absolute and relative, for solving antenna parameter tuning tasks. We consider two qualitatively different problems, optimization for

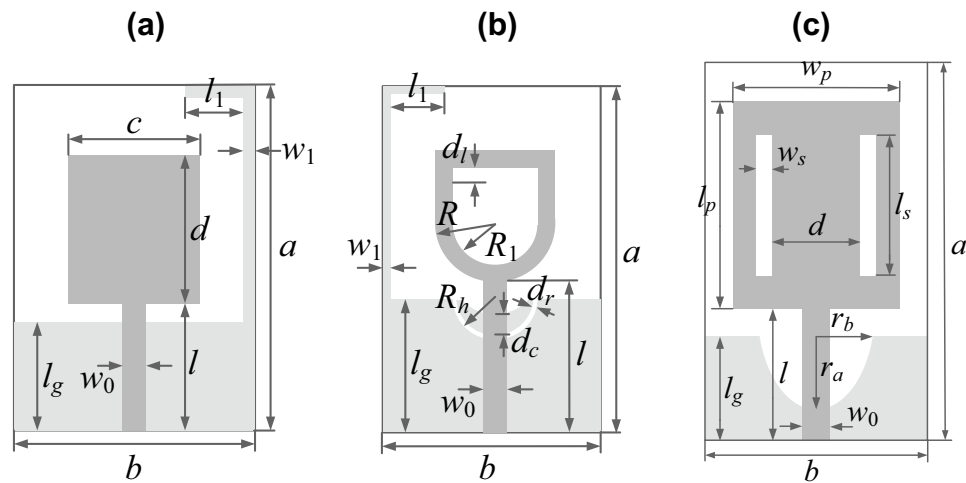


Figure 2. Benchmark antenna structures: (a) Antenna I⁶⁰, (b) Antenna II⁶¹, (c) Antenna III⁵⁵. Ground planes marked using light gray shade. (Microsoft Visio 2016, <https://www.microsoft.com/pl-pl/microsoft-365/visio/>).

minimum size, and optimization for best in-band matching. As mentioned before, these problems have entirely different characteristics, e.g., size reduction features smooth primary objective and expensive constraints, whereas reflection improvement task uses expensive (EM-evaluated) objective and geometry-only constraints. As demonstrated below, antenna parameterization is of paramount importance from the point of view of the optimization process performance.

Benchmark antenna structures and parameterizations. The numerical studies are carried out using three broadband monopole antennas shown in Fig. 2. All structures are to operate within UWB band of 3.1 GHz to 10.6 GHz. Antennas I⁶⁰ and II⁶¹ are implemented on RF-35 substrate ($\epsilon_r = 3.5$, $h = 0.762$ mm), whereas Antenna III⁵⁵ is implemented on FR4 substrate ($\epsilon_r = 4.3$, $h = 1.55$ mm). The feed lines widths (parameter w_0) are dimensioned to ensure 50- Ω input impedance: we have $w_0 = 1.7$ mm for Antenna I and II, and $w_0 = 3.0$ mm for Antenna III. The EM models are evaluated using time-domain solver of CST Microwave Studio. The models include the SMA connectors. In all cases, metallization is represented as perfect electrical conductor (PEC), whereas dielectric losses are taken into account.

For each antenna, we consider two parameterizations, the absolute and the relative one (cf. “Geometry parameterization: Absolute vs. relative”). The details concerning both parameterizations for Antenna I, II, and III are provided in Table 3, which also contains information about additional geometry constraints as well as the relationships between the antenna dimensions and design variables.

The work focuses on establishing antenna parameterization for the purpose of design optimization. Thus, experimental validation of the designs of the considered antenna structures has not been provided as it is immaterial to the topic of the paper. Moreover, all of the considered structures have been already validated in the respective source papers^{55,60,61}, but also in our previous works where their numerical optimization has been performed^{49,62,63}.

Numerical experiments: setup. In order to evaluate the merits of the considered antenna parameterizations, we carry out optimization of the structures of Fig. 2 under the following two scenarios:

- Optimization for matching improvement in the UWB frequency range, in which case, the objective function is of the form $U(\mathbf{x}) = \max\{3.1 \text{ GHz} \leq f \leq 10.6 \text{ GHz} : |S_{11}(\mathbf{x}, f)|\}$;
- Optimization for size reduction; the objective function is of the form $U(\mathbf{x}) = A(\mathbf{x})$. Furthermore, the condition $S(\mathbf{x}) \leq -10$ dB is imposed on the reflection response, where $S(\mathbf{x}) = \max\{3.1 \text{ GHz} \leq f \leq 10.6 \text{ GHz} : |S_{11}(\mathbf{x}, f)|\}$. The constraint is handled implicitly as in (3) with the penalty function of the form $c(\mathbf{x}) = [(S(\mathbf{x}) + 10)/10]^2$. For all considered structures, the size is understood as the area of the entire substrate containing the antenna.

The optimization algorithm of choice is trust-region gradient search with numerical derivatives⁶², which produces a series of approximations to the optimal design \mathbf{x}^* using an auxiliary linear expansion model of antenna responses established at the iteration point. More details about the procedure can be found in the literature^{63,64}.

For each design scenario, the optimization process is executed ten times from random initial designs (the same starting points are used in both scenarios). This is to account for the fact that the optimization problem might be multimodal due to a relatively large number of parameters as well as the presence of numerical noise. For both reasons, the final design generally depends on the starting point; consequently, evaluating performance of the algorithm based on a single run is not representative.

The following metrics are used:

Antenna	Parameterization	
	Absolute	Relative
I		
Independent parameters	$\mathbf{x} = [a \ b \ l \ c \ d \ l_g \ l_1 \ w_1]^T$	$\mathbf{x} = [l \ c \ d \ d_1 \ d_w \ l_{gr} \ l_r \ w_1]^T$
Additional constraints	$l + d \leq a; d \leq b; l_g \leq a - w_1; l_1 + w_1 \leq b$	None
Additional relationships	None	$a = l + d + d_1; b = 2d_w + c;$ $l_g = l_{gr}(a - w_1); l_1 = l_r(b - w_1)$
II		
Independent parameters	$\mathbf{x} = [a \ b \ l \ d_1 \ R \ R_1 \ l_g \ l_1 \ R_h \ d_r \ d_c \ w_1]^T$	$\mathbf{x} = [l \ d_1 \ R \ R_1 \ r \ d_a \ d_b \ l_{gr} \ l_r \ R_{hr} \ d_{rr} \ d_{cr} \ w_1]^T$
Additional constraints	$l + 3R - R_1 + d_1 \leq a; 2R \leq b; R_1 \leq R;$ $d_r \leq R_h; w_1 + l_1 \leq b;$ $l_g \leq a - w_1; d_c \leq R_h - d_r$	None
Additional relationships	None	$R_1 = R_1 R; a = l + 3R - R_1 + d_1 + d_a;$ $l_g = l_{gr}(a - w_1); l_1 = l_r(b - w_1);$ $R_h = R_{hr} b/2; d_r = d_{rr} R_h;$ $d_c = d_{cr}(R_h - d_r) + d_r$
III		
Independent parameters	$\mathbf{x} = [a \ b \ l \ l_p \ w_p \ l_s \ w_s \ d \ l_g \ r_a \ r_b]^T$	$\mathbf{x} = [l_{gr} \ l \ l_s \ w \ d \ d_a \ d_b \ d_w \ r_{ar} \ r_{br}]^T$
Additional constraints	$w_p \leq b; 2w_s + d \leq w_p; l + l_p \leq a;$ $l_s \leq l_p; 2r_b \leq b; r_a \leq l_g$	None
Additional relationships	None	$a = l + l_p + d_a; b = d + 2w_s + 2d_{ws} + 2d_b;$ $l_p = l_s + 2d_{ls}; w_p = d + 2w_s + 2d_{ws};$ $l_g = l_{gr} a; r_a = r_{ar} l_g; r_b = r_{br} b/2$

Table 3. Parameterization of Antenna I, II, and III (Fig. 2).

Antenna	Optimization scenario	Performance metric	I		II		III	
			Absolute	Relative	Absolute	Relative	Absolute	Relative
Matching improvement		$U(\mathbf{x}^*)^1$ (dB)	-12.2	-12.0	-13.3	-14.7	-9.9	-11.5
		Std[$U(\mathbf{x}^*)$] (dB)	0.8	0.6	0.6	0.5	1.8	0.5
		Cost ⁴	88.5	89.4	126.1	126.3	139.9	146.3
Size reduction		Footprint area $A(\mathbf{x}^*)^2$ (mm ²)	316.9	328.8	246.5	295.9	199.7	212.8
		Std[$A(\mathbf{x}^*)$]	36.5	30.4	19.4	37.1	16.1	14.2
		Constraint violation D^3 (dB)	0.9	0.9	0.4	1.0	0.9	0.9
		Std[D] (dB)	0.9	0.7	0.3	0.4	0.3	0.3
		Cost ⁴	112.2	103.5	191.3	176.8	163.6	164.9

Table 4. Optimization results of Antennas I through III. ¹Optimized maximum in-band reflection, averaged over ten algorithm runs. ²Optimized antenna footprint averaged over ten algorithm runs. ³Constraint violation, defined as $D = \{3.1 \text{ GHz} \leq f \leq 10.6 \text{ GHz} : \max |S_{11}(f)|\} + 10$, averaged over ten algorithm runs. ⁴Number of EM simulations averaged over ten algorithm runs.

- Optimization for matching improvement: maximum in-band reflection, the value averaged over ten algorithm runs as well as the standard deviation;
- Optimization for size reduction: obtained footprint area (average and standard deviation), as well as violation of the reflection constraint $S(x) \leq -10$ dB (average value and the standard deviation);

Comparison of the aforementioned factors for both antenna parameterizations will provide meaningful assessment of the optimization process performance and reliability.

Numerical experiments: results and discussion. Table 4 provides the numerical results for Antennas I, II, and III, respectively. Furthermore, Fig. 3 illustrates the initial and optimized designs for the selected algorithm runs, whereas Table 5 gathers the respective geometry parameter vectors. Figure 4 shows the comparison of the average in-band reflection level and the footprint area for the considered antennas optimized using the absolute and relative parameterizations.

The results allow us to draw several conclusions concerning the performance of the optimization process, depending on the parameterization used. These can be summarized as follows:

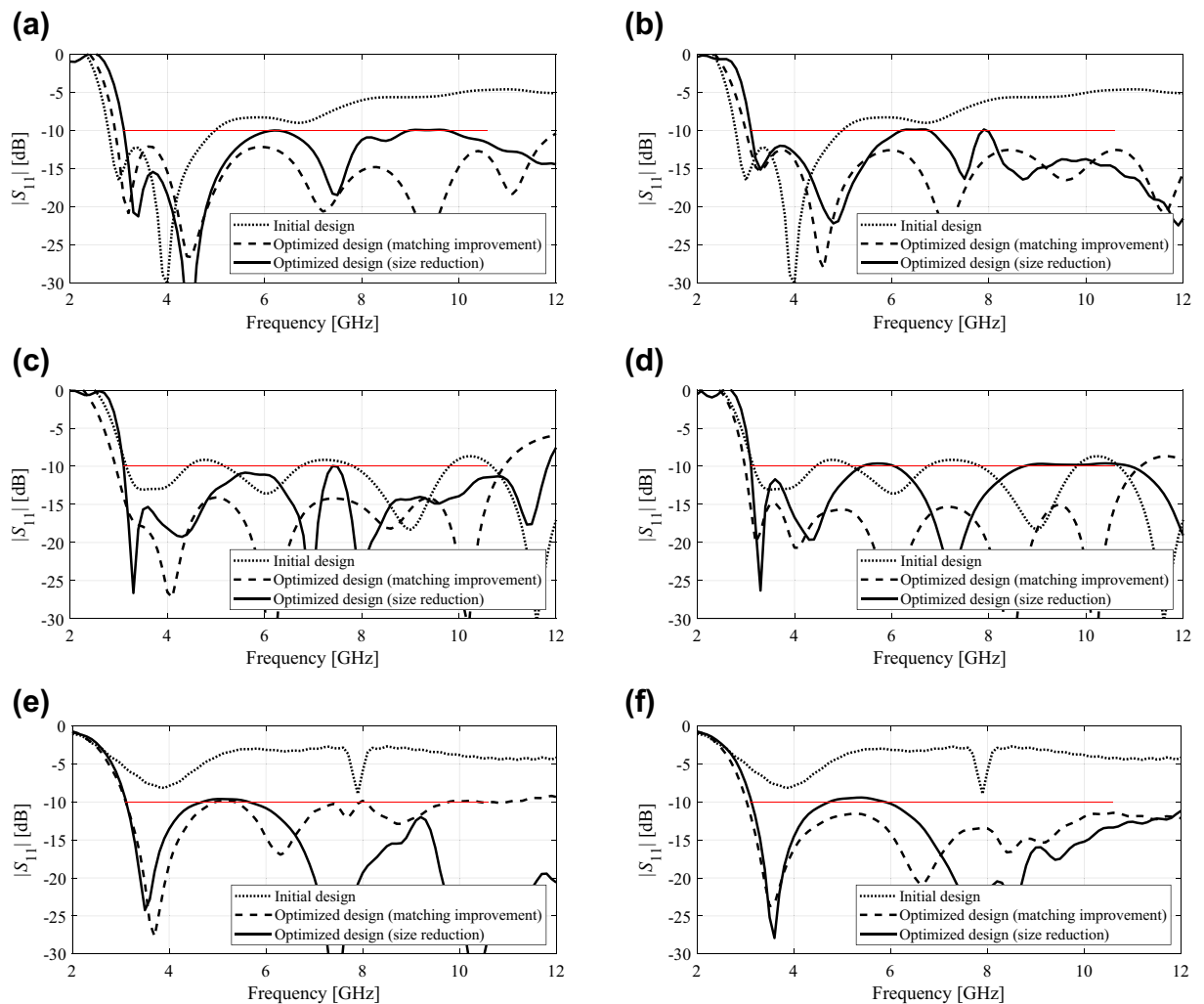


Figure 3. Selected optimization runs for Antennas I through III (see also Table 5): initial design (\cdots), design \mathbf{x}^1 optimized for best matching, ($- - -$), design \mathbf{x}^2 optimized for minimum size ($-$); Antenna I: (a) absolute parameterization ($S(\mathbf{x}^1) = -12.4$ dB, $A(\mathbf{x}^2) = 278$ mm²), (b) relative parameterization ($S(\mathbf{x}^1) = -12.2$ dB, $A(\mathbf{x}^2) = 300$ mm²); Antenna II: (c) absolute parameterization ($S(\mathbf{x}^1) = -14.0$ dB, $A(\mathbf{x}^2) = 225$ mm²), (d) relative parameterization ($S(\mathbf{x}^1) = -14.9$ dB, $A(\mathbf{x}^2) = 293$ mm²); Antenna III: (e) absolute parameterization ($S(\mathbf{x}^1) = -10.0$ dB, $A(\mathbf{x}^2) = 201$ mm²), (f) relative parameterization ($S(\mathbf{x}^1) = -11.4$ dB, $A(\mathbf{x}^2) = 229$ mm²). Design specifications for antenna reflection marked using a horizontal line. (Matlab R2016a <https://www.mathworks.com>).

- When optimizing for improvement of the in-band matching, relative parameterization is noticeably better (or at least comparable with the absolute one in the case of Antenna I). For Antennas II and III, relative parameterization yields the designs that are better by about 1.5 dB on the average;
- At the same time, repeatability of results is improved for relative parameterization as compared to the absolute one, which is indicated by a generally smaller values of the standard deviation of the objective function;
- When optimizing for minimum size, absolute parameterization is consistently better than the relative one. The improvement is as high as 25 mm² on the average, which is about ten percent in relative terms;
- Repeatability of solutions when optimizing for size reduction is similar for both parameterizations although slightly in favor of the absolute one on the average;
- The average reflection constraint violation (when optimizing for size reduction) is similar for both parameterizations. It should be noted at this point that the level of violation is controlled by the penalty coefficient β (cf. (3)), which was set to 10^3 in all cases. Increasing this value would reduce the average violations while being detrimental to the obtained size reduction⁶⁵.
- The computational cost of the optimization process is consistent for both parameterizations, the differences are statistically insignificant. It can also be observed that the expenses associated with size reduction are higher than those required for matching improvement, which is due to the fact that the former task is a constrained one with nonlinear inequality constraint; thus the problem is numerically more demanding. Also, it can be observed that the computational complexity is more or less proportional to the dimensionality of the parameter space, which is expected for gradient-based trust region procedures with numerical derivatives.

Antenna	Parameterization	Design scenario	Geometry parameter values (mm)												
I	Absolute		a	b	l	c	d	l_g	l_1	w_1					
		Best matching	22.31	19.10	7.00	10.36	9.64	6.10	3.34	2.16					
		Size reduction	19.11	14.54	6.61	8.92	8.49	6.02	6.79	2.29					
	Relative		l	c	d	d_l	d_w	l_{gr}	l_{1r}	w_1					
		Best matching	6.52	10.82	10.41	5.34	4.58	0.28	0.17	2.22					
II	Absolute		a	b	l	d_l	R	R_1	l_g	l_1	R_h	d_r	d_c	w_1	
		Best matching	25.00	19.94	9.58	0.39	5.33	1.50	9.68	4.26	2.54	0.42	1.23	1.11	
		Size reduction	21.04	10.73	7.78	0.51	4.30	2.55	8.31	6.00	3.16	0.44	2.35	0.50	
	Relative		l	d_l	R	R_1	d_a	d_b	l_{gr}	l_{1r}	R_{hr}	d_{rr}	d_{cr}	w_1	
		Best matching	10.10	0.39	5.40	0.26	2.14	6.15	10.06	0.22	0.21	0.11	0.79	0.63	
III	Absolute		a	b	l	l_p	w_p	l_s	w_s	d	l_g	r_a	r_b		
		Best matching	30.66	16.27	11.33	13.63	6.56	11.39	0.64	4.05	9.20	1.88	1.57		
		Size reduction	23.07	8.70	13.27	9.64	8.70	9.11	0.76	1.54	9.45	3.06	4.19		
	Relative		l_{gr}	l	l_s	w_s	d	d_a	d_b	d_{ws}	d_w	r_{ar}	r_{br}		
		Best matching	8.78	12.32	10.62	0.20	5.05	5.45	0.69	0.58	3.58	0.24	0.41		
		Size reduction	9.23	11.82	9.87	0.49	5.11	2.49	0.49	0.78	0.73	0.80	0.41		

Table 5. Optimized geometry parameter vectors for the designs of Fig. 3.

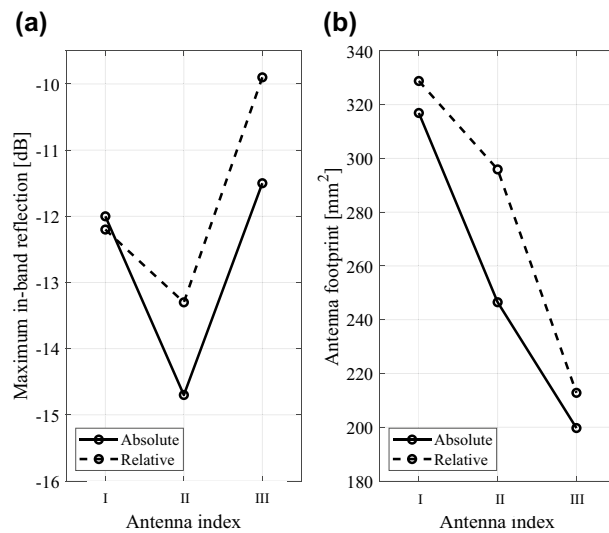


Figure 4. Comparison of the optimization process performance between the absolute (—) and relative (---) antenna parameterization. Shown are: (a) the maximum in-band reflection of the antenna, averaged over the ten independent optimization runs (optimization for matching improvement), and (b) antenna footprint area averaged over the ten independent optimization runs (optimization for size reduction). Consistent differences between the two parameterization can be observed, in favor of relative parameterization when optimizing for matching improvement, and absolute parameterization when optimizing for size reduction. (Matlab R2016a <https://www.mathworks.com>).

The overall conclusion is that the performance of the optimization process demonstrably depends on the parameterization. Based on the numerical experiments presented in this section, the absolute parameterization is shown to be more suitable for solving size reduction tasks, whereas relative parameterization is more beneficial when optimizing electrical characteristics of the antenna. Here, additional studies will be necessary to investigate the properties of both parameterizations, especially when handling other types of antenna responses (axial ratio, gain, etc.), or carrying out size reduction under multiple constraints. Notwithstanding, the results obtained in this work provide a clear indication of the importance of geometry parameterization in the optimization context. Furthermore, although our studies were conducted for local parameter tuning (here, using a gradient search algorithm), selecting parameterization has further reaching consequences when considering other optimization frameworks. For example, eliminating geometry constraints (both linear and nonlinear) as

Optimization scenario	Performance metric	Parameterization	
		Absolute	Relative
Gain variability minimization	$U(\mathbf{x}^*)^1$ [dB]	1.58	2.31
	$\text{Std}[U(\mathbf{x}^*)]$ [dB]	0.44	0.69
	Cost ²	94.0	86.8

Table 6. Gain variability minimization results for Antenna I. ¹Optimized in-band gain variability, averaged over ten algorithm runs. ²Number of EM simulations averaged over ten algorithm runs.

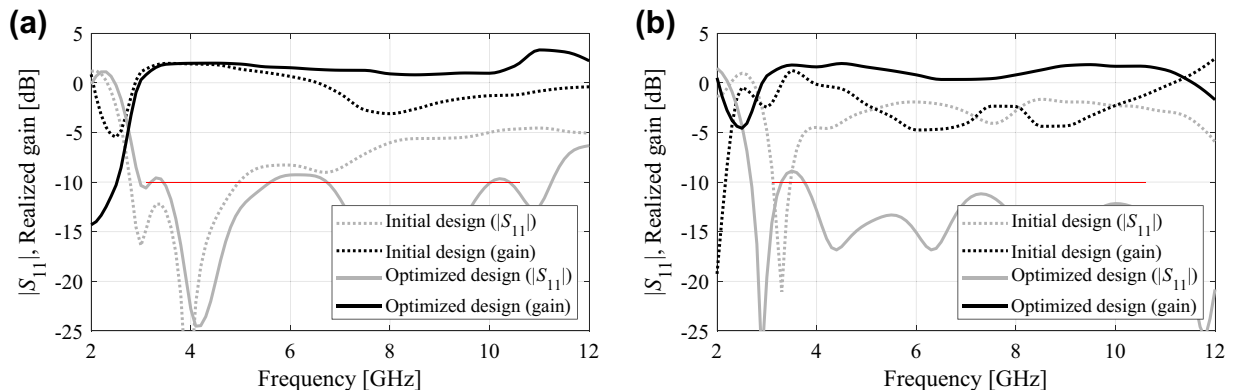


Figure 5. Selected optimization runs for Antenna I oriented towards gain variability reduction (cf. Table 6): initial design (\cdots), design optimized for minimum gain variability, ($-$), (a) absolute parameterization (gain variability 1.2 dB), (b) relative parameterization (gain variability 1.7 dB). Reflection and realized gain characteristics shown using gray and black lines, respectively. (Matlab R2016a <https://www.mathworks.com>).

in relative parameterization facilitates utilization of nature-inspired algorithms for which the ‘natural’ environment is a box-constrained domain.

The reasons for superiority of absolute parameterization over the relative one for matching improvement, and quite the opposite performance for size reduction are not clear at this point. It seems that one of the factors is that the primary objective in size reduction task is a smooth function of geometry parameters, whereas the boundary of the feasible region is determined by the EM-evaluated condition (i.e., inherently noisy). In this setup, the additional constraints pertinent to absolute parameterization do not aggravate the problem because of being smooth as well. On the other hand, absolute parameters give a more direct account for antenna size, which is not the case for relative parameterization. When optimizing for best matching, the latter factor is not as important, whereas the necessity of handling constraints might be detrimental to the quality of the optimization outcome and, therefore, give an edge to the relative parameterization.

Although in this work we focused on two specific optimization tasks: matching improvement and size reduction, a similar analysis can be made for other types of problems. This will be the subject of the future work; however, to emphasize the general importance of parameterization, an additional set of experiments has been performed for Antenna I, which is reduction of in-band realized gain variability. Here, the objective function to be minimized is defined as $U(\mathbf{x}) = \max\{3.1 \text{ GHz} \leq f \leq 10.6 \text{ GHz} : |G(\mathbf{x}, f)|\} - \min\{3.1 \text{ GHz} \leq f \leq 10.6 \text{ GHz} : |G(\mathbf{x}, f)|\}$, where $G(\mathbf{x}, f)$ is a broadside realized gain at the design \mathbf{x} and frequency f . The task is subject to constraint $S(\mathbf{x}) \leq -10 \text{ dB}$, $S(\mathbf{x}) = \max\{3.1 \text{ GHz} \leq f \leq 10.6 \text{ GHz} : |S_{11}(\mathbf{x}, f)|\}$. Similarly, as for the size reduction task, it is handled implicitly (cf. (3)) with the penalty function of the form $c(\mathbf{x}) = [(S(\mathbf{x}) + 10)/10]^2$; in this case, we use small value of the penalty coefficient to foster the improvement of the primary objective at the expense of tolerating certain violation of the reflection constraint. The reason for considering this particular problem is that stable gain is important for broadband antennas, yet it is difficult to achieve. Numerical optimization turns instrumental here.

Table 6 provides numerical results in terms of the average in-band gain variability, its standard deviation, as well as the computational cost of the optimization process. Figure 5 shows antenna responses for the selected algorithm runs. The parameter vectors corresponding to the optimized design of Fig. 5 are $\mathbf{x}^1 = [21.21 \ 14.97 \ 6.26 \ 11.04 \ 11.12 \ 4.87 \ 3.73 \ 0.40]^T$ (absolute parameterization) and $\mathbf{x}^2 = [7.33 \ 11.06 \ 10.50 \ 1.71 \ 6.70 \ 0.37 \ 0.20 \ 2.40]^T$ (relative parameterization). It can be observed that absolute parameterization is more advantageous for handling gain characteristics. The obtained gain variability lower by over 0.7 dB on the average than for relative parameterization; the standard deviation is noticeably smaller as well. At the same time, the computational costs of the optimization process are comparable for both parameterizations, which is consistent with the results contained in Table 4.

Conclusion

This paper investigated the issue of geometry parameterization in the context of EM-driven parameter tuning of antenna structures. The two types thereof were considered, the absolute (all antenna dimensions expressed in the appropriate length units, e.g., millimetres), and the relative one with the sizes of the structure components expressed in relation the size of encapsulating elements. The qualitative merits of both parameterizations were discussed, followed by comprehensive numerical experiments carried out using three broadband antennas. At the level of the optimization problem formulation, the advantage of absolute parameterization is its simplicity, which comes at the expense of being accompanied by a number of constraints necessary to ensure the geometrical consistency of the structure. On the other hand, relative parameterization eliminates the need for additional constraints making the problem domain as simple as an interval (i.e., parameter space defined using only lower and upper bounds for the parameters).

The numerical results obtained for two design scenarios (optimization for minimum size and best matching) with the optimization executed multiple times from random initial designs, indicate that the performance of the EM-driven design process is affected by the choice of parameterization to a great extent. In particular, absolute parameterization turns out to be more suitable for solving size reduction tasks, whereas relative parameterization is favoured for handling electrical characteristics (here, represented by the in-band matching improvement task). The performance differences are quite significant: the average maximum in-band matching is better by 1.5 dB when using absolute versus relative sizing, whereas relative parameterization leads to size reduction better by 25 mm² (or about ten percent) as compared to the absolute one (again, when averaged over all algorithm runs and all considered antenna structures).

The reasons for these differences seem to be related to whether a particular task is formulated as a constrained or unconstrained one, but also to whether the primary objective is computationally cheap (as in size reduction tasks) or expensive (as when handling antenna electrical characteristics). An additional reason might be related to the overall objective function landscape, which favours absolute parameterization when the goal is related to the physical size of the antenna, yet fosters relative dimension sizing in other cases. More experiments are needed to determine a suitability of particular ways of parameterizing antenna geometry across a broader range of EM-driven design tasks, which will be the subject of the future work.

Received: 16 July 2021; Accepted: 8 December 2021

Published online: 21 December 2021

References

- Zhang, Y., Deng, J., Li, M., Sun, D. & Guo, L. A MIMO dielectric resonator antenna with improved isolation for 5G mm-wave applications. *IEEE Ant. Wirel. Propag. Lett.* **18**, 747–751 (2019).
- Samadi Taheri, M. M., Abdipour, A., Zhang, S. & Pedersen, G. F. Integrated millimeter-wave wideband end-fire 5G beam steerable array and low-frequency 4G LTE antenna in mobile terminals. *IEEE Trans. Veh. Techn.* **68**, 4042–4046 (2019).
- Manshari, S., Koziel, S. & Leifsson, L. Compact dual-polarized corrugated horn antenna for satellite communications. *IEEE Trans. Antennas Propag.* **68**, 5122–5129 (2020).
- Yang, X., Ge, L., Wang, J. & Sim, C. A differentially driven dual-polarized high-gain stacked patch antenna. *IEEE Ant. Wirel. Propag. Lett.* **17**, 1181–1185 (2018).
- Sang, L., Wu, S., Liu, G., Wang, J. & Huang, W. High-gain UWB Vivaldi antenna loaded with reconfigurable 3-D phase adjusting unit lens. *IEEE Ant. Wirel. Propag. Lett.* **19**, 322–326 (2020).
- Assimonis, S. D., Abbasi, M. A. B. & Fusco, V. Millimeter-wave multi-mode circular antenna array for uni-cast multi-cast and OAM communication. *Sci. Rep.* **11**, 4928 (2021).
- Li, S., Wang, S., An, Q., Zhao, G. & Sun, H. Cylindrical MIMO array-based near-field microwave imaging. *IEEE Trans. Antennas Propag.* **69**, 612–617 (2021).
- Wu, T., Li, R. & Tentzeris, M. M. A scalable solar antenna for autonomous integrated wireless sensor nodes. *IEEE Ant. Wirel. Propag. Lett.* **10**, 510–513 (2011).
- Valanarasi, A. & Dhanasekaran, R. Optimum band ϵ shaped miniature implantable antennas for telemetry applications. *IEEE Trans. Antennas Propag.* **69**, 55–63 (2021).
- Yuan, X. *et al.* Ultra-wideband MIMO antenna system with high element-isolation for 5G smartphone application. *IEEE Access* **8**, 56281–56289 (2020).
- Cai, Z., Zhou, Y., Qi, Y., Zhuang, W. & Deng, L. A millimeter wave dual-lens antenna for IoT-based smart parking radar system. *IEEE Internet of Things J.* **8**, 418–427 (2021).
- Rahman, A., Islam, M., Singh, M., Kibria, S. & Khtaruzzaman, M. Electromagnetic performances analysis of an ultra-wideband and flexible material antenna in microwave breast imaging: To implement a wearable medical bra. *Sci. Rep.* **6**, 38906 (2016).
- Afifi, A. I., Abdel-Rahman, A. B., El-Hameed, A. S. A., Allam, A. & Ahmed, S. M. Small frequency ratio multi-band dielectric resonator antenna utilizing vertical metallic strip pairs feeding structure. *IEEE Access* **8**, 112840–112845 (2020).
- Houret, T., Lizzi, L., Ferrero, F., Danchesi, C. & Boudaud, S. DTC-enabled frequency-tunable inverted-F antenna for IoT applications. *IEEE Ant. Wirel. Propag. Lett.* **19**, 307–311 (2020).
- Zhang, Y., Wang, H., Liao, D. & Fu, W. Phase-tuning metasurface for circularly polarized broadside radiation in broadband. *Sci. Rep.* **8**, 2970 (2018).
- Liang, Z., Lv, S., Li, Y., Liu, J. & Long, Y. Compact folded slot antenna and its endfire arrays with high gain and vertical polarization. *IEEE Ant. Wirel. Propag. Lett.* **19**, 786–790 (2020).
- Lalbahsh, A., Afzal, M. U., Hayat, T., Esselle, K. P. & Mandal, K. All-metal wideband metasurface for near-field transformation of medium-to-high gain electromagnetic sources. *Sci. Rep.* **11**, 9421 (2021).
- Yang, G., Zhang, Y. & Zhang, S. Wide-band and wide-angle scanning phased array antenna for mobile communication system. *IEEE Open J. Antennas Propag.* **2**, 203–212 (2021).
- Ren, J., Hu, W., Yin, Y. & Fan, R. Compact printed MIMO antenna for UWB applications. *IEEE Ant. Wirel. Propag. Lett.* **13**, 1517–1520 (2014).
- Tao, J. & Feng, Q. Compact ultrawideband MIMO antenna with half-slot structure. *IEEE Ant. Wirel. Propag. Lett.* **16**, 792–795 (2017).
- Reddy, B. R. S. & Vakula, D. Compact zigzag-shaped-slit microstrip antenna with circular defected ground structure for wireless applications. *IEEE Ant. Wirel. Propag. Lett.* **14**, 678–681 (2015).

22. Wang, Z., Li, C. & Yin, Y. A meta-surface antenna array decoupling (MAAD) design to improve the isolation performance in a MIMO system. *IEEE Access* **8**, 61797–61805 (2020).
23. Roshna, T. K., Deepak, U., Sajitha, V. R., Vasudevan, K. & Mohanan, P. A compact UWB MIMO antenna with reflector to enhance isolation. *IEEE Trans. Antennas Propag.* **63**, 1873–1877 (2015).
24. Liu, J., Esselle, K. P., Hay, S. G. & Zhong, S. Effects of printed UWB antenna miniaturization on pulse fidelity and pattern stability. *IEEE Trans. Antennas Propag.* **62**, 3903–3910 (2014).
25. Hassan, E., Noreland, D., Augustine, R., Wadbro, E. & Berggren, M. Topology optimization of planar antennas for wideband near-field coupling. *IEEE Trans. Antennas Propag.* **63**, 4208–4213 (2015).
26. Koziel, S. & Pietrenko-Dabrowska, A. Expedited optimization of antenna input characteristics with adaptive Broyden updates. *Eng. Comp.* **37**, 851–862 (2019).
27. Koziel, S., Bekasiewicz, A., Couckuyt, I. & Dhaene, T. Efficient multi-objective simulation-driven antenna design using co-kriging. *IEEE Trans. Antennas Propag.* **62**, 5900–5905 (2014).
28. Barmuta, P., Ferranti, F., Gibiino, G. P., Lewandowski, A. & Schreurs, D. M. M. P. Compact behavioral models of nonlinear active devices using response surface methodology. *IEEE Trans. Microw. Theory Techn.* **63**, 56–64 (2015).
29. Ghorbani, F. et al. Deep neural network-based automatic metasurface design with a wide frequency range. *Sci. Rep.* **11**, 7102 (2021).
30. Jacobs, J. P. & Koziel, S. Two-stage framework for efficient Gaussian process modeling of antenna input characteristics. *IEEE Trans. Antennas Propag.* **62**, 706–713 (2014).
31. Polikar, R. Ensemble learning. In *Ensemble Machine Learning* (eds Zhang, C. & Ma, Y.) 1–34 (Springer, 2012).
32. Baratta, I. A., de Andrade, C. B., de Assis, R. R. & Silva, E. J. Infinitesimal dipole model using space mapping optimization for antenna placement. *IEEE Ant. Wirel. Propag. Lett.* **17**, 17–20 (2018).
33. Su, Y., Li, J., Fan, Z. & Chen, R. Shaping optimization of double reflector antenna based on manifold mapping. *Int. Applied Comp. Electromagnetics Soc. Symp. (ACES)*, Suzhou, China, 1–2 (2017).
34. Koziel, S. & Unnsteinsson, S. D. Expedited design closure of antennas by means of trust-region-based adaptive response scaling. *IEEE Ant. Wirel. Propag. Lett.* **17**, 1099–1103 (2018).
35. Koziel, S. & Leifsson, L. *Simulation-Driven Design by Knowledge-Based Response Correction Techniques* (Springer, 2016).
36. Zhang, C., Feng, F., Gongal-Reddy, V., Zhang, Q. J. & Bandler, J. W. Cognition-driven formulation of space mapping for equal-ripple optimization of microwave filters. *IEEE Trans. Microw. Theory Techn.* **63**, 2154–2165 (2015).
37. Tak, J., Kantemur, A., Sharma, Y. & Xin, H. A 3-D-printed W-band slotted waveguide array antenna optimized using machine learning. *IEEE Ant. Wirel. Propag. Lett.* **17**, 2008–2012 (2018).
38. Liu, B., Koziel, S. & Ali, N. SADEA-II: A generalized method for efficient global optimization of antenna design. *J. Comp. Design Eng.* **4**, 86–97 (2017).
39. Lim, D. K. et al. A novel surrogate-assisted multi-objective optimization algorithm for an electromagnetic machine design. *IEEE Trans. Magn.* **51**, 8200804 (2015).
40. Dong, J., Qin, W. & Wang, M. Fast multi-objective optimization of multi-parameter antenna structures based on improved BPNN surrogate model. *IEEE Access* **7**, 77692–77701 (2019).
41. Xiao, S. et al. Multi-objective Pareto optimization of electromagnetic devices exploiting kriging with Lipschitzian optimized expected improvement. *IEEE Trans. Magn.* **54**, 7001704 (2018).
42. Koziel, S., Cheng, Q. S. & Li, S. Optimization-driven antenna design framework with multiple performance constraints. *Int. J. RF Microw. CAE* **28**, e21208 (2018).
43. Yücel, A. C., Bağcı, H. & Michielssen, E. An ME-PC enhanced HDMR method for efficient statistical analysis of multiconductor transmission line networks. *IEEE Trans. Comp. Packaging Manufact. Techn.* **5**, 685–696 (2015).
44. Koziel, S. & Pietrenko-Dabrowska, A. Fast multi-objective optimization of antenna structures by means of data-driven surrogates and dimensionality reduction. *IEEE Access* **8**, 183300–183311 (2020).
45. Spina, D., Ferranti, F., Antonini, G., Dhaene, T. & Knockaert, L. Efficient variability analysis of electromagnetic systems via polynomial chaos and model order reduction. *IEEE Trans. Comp. Packaging Manufact. Techn.* **4**, 1038–1051 (2014).
46. Li, X. Finding deterministic solution from underdetermined equation: Large-scale performance modeling of analog/RF circuits. *IEEE Trans. Comput. Aided Des. Integr. Circuits Syst.* **29**, 1661–1668 (2010).
47. Hu, R., Monebhurrun, V., Himeno, R., Yokota, H. & Costen, F. An adaptive least angle regression method for uncertainty quantification in FDTD computation. *IEEE Trans. Antennas Propag.* **66**, 7188–7197 (2018).
48. Easum, J. A., Nagar, J., Werner, P. L. & Werner, D. H. Efficient multi-objective antenna optimization with tolerance analysis through the use of surrogate models. *IEEE Trans. Antennas Propag.* **66**, 6706–6715 (2018).
49. Tomasson, J. A., Koziel, S. & Pietrenko-Dabrowska, A. Quasi-global optimization of antenna structures using principal components and affine subspace-spanned surrogates. *IEEE Access* **8**, 50078–50084 (2020).
50. Koziel, S. Fast simulation-driven antenna design using response-feature surrogates. *Int. J. RF Microw. CAE* **25**, 394–402 (2015).
51. Koziel, S. & Pietrenko-Dabrowska, A. Expedited feature-based quasi-global optimization of multi-band antennas with Jacobian variability tracking. *IEEE Access* **8**, 83907–83915 (2020).
52. Petrocchi, A. et al. Measurement uncertainty propagation in transistor model parameters via polynomial chaos expansion. *IEEE Microw. Wirel. Comp. Lett.* **27**, 572–574 (2017).
53. Du, J. & Roblin, C. Statistical modeling of disturbed antennas based on the polynomial chaos expansion. *IEEE Ant. Wirel. Prop. Lett.* **16**, 1843–1847 (2017).
54. Koziel, S. Objective relaxation algorithm for reliable simulation-driven size reduction of antenna structure. *IEEE Ant. Wirel. Propag. Lett.* **16**, 1949–1952 (2017).
55. Haq, M. A. & Koziel, S. Simulation-based optimization for rigorous assessment of ground plane modifications in compact UWB antenna design. *Int. J. RF Microw. CAE* **28**, e21204 (2018).
56. Chen, Q., Ding, J., Yang, S. & Chai, T. A novel evolutionary algorithm for dynamic constrained multiobjective optimization problems. *IEEE Trans. Evol. Comp.* **24**, 792–806 (2020).
57. Feng, Q., Li, Q., Wang, H., Feng, Y. & Pan, Y. Two-stage adaptive constrained particle swarm optimization based on bi-objective method. *IEEE Access* **8**, 150647–150664 (2020).
58. Xu, B. & Zhang, Z. Constrained optimization based on ensemble differential evolution and two-level-based epsilon method. *IEEE Access* **8**, 213981–213997 (2020).
59. Koziel, S. & Ogurtsov, S. *Antenna Design by Simulation-Driven Optimization. Surrogate-Based Approach* (Springer, 2014).
60. Koziel, S. & Bekasiewicz, A. Low-cost multi-objective optimization of antennas using Pareto front exploration and response features. *Int. Symp. Antennas Prop. Fajardo, Puerto Rico* (2016).
61. Alsath, M. G. N. & Kanagasabai, M. Compact UWB monopole antenna for automotive communications. *IEEE Trans. Antennas Propag.* **63**, 4204–4208 (2015).
62. Koziel, S. & Pietrenko-Dabrowska, A. Reduced-cost design closure of antennas by means of gradient search with restricted sensitivity update. *Metrol. Meas. Syst.* **26**, 595–605 (2019).
63. Koziel, S. & Pietrenko-Dabrowska, A. Reduced-cost electromagnetic-driven optimization of antenna structures by means of trust-region gradient-search with sparse Jacobian updates. *IET Microw. Antennas Propag.* **13**, 1646–1652 (2019).
64. Conn, A. R., Gould, N. I. M. & Toint, P. L. *Trust Region Methods* (SIAM, 2000).

65. Johansson, D. O. & Koziel, S. Feasible space boundary search for improved optimization-based miniaturization of antenna structures. *IET Microw. Antennas Propag.* **12**, 1273–1278 (2018).

Acknowledgements

The authors would like to thank Dassault Systemes, France, for making CST Microwave Studio available. This work is partially supported by the Icelandic Centre for Research (RANNIS) Grant 217771 and by Gdańsk University of Technology Grant DEC-41/2020/IDUB/I.3.3 under the Argentum Triggering Research Grants program—'Excellence Initiative—Research University'.

Author contributions

Conceptualization, S.K. and A.P.; methodology, S.K. and A.P.; software, S.K. and A.P.; validation, S.K. and A.P.; formal analysis, S.K.; investigation, S.K. and A.P.; resources, S.K.; data curation, S.K. and A.P.; writing—original draft preparation, S.K. and A.P.; writing—review and editing, S.K.; visualization, S.K. and A.P.; supervision, S.K.; project administration, S.K.; funding acquisition, S.K. All authors reviewed the manuscript.

Competing interests

The authors declare no competing interests.

Additional information

Correspondence and requests for materials should be addressed to A.P.-D.

Reprints and permissions information is available at www.nature.com/reprints.

Publisher's note Springer Nature remains neutral with regard to jurisdictional claims in published maps and institutional affiliations.



Open Access This article is licensed under a Creative Commons Attribution 4.0 International License, which permits use, sharing, adaptation, distribution and reproduction in any medium or format, as long as you give appropriate credit to the original author(s) and the source, provide a link to the Creative Commons licence, and indicate if changes were made. The images or other third party material in this article are included in the article's Creative Commons licence, unless indicated otherwise in a credit line to the material. If material is not included in the article's Creative Commons licence and your intended use is not permitted by statutory regulation or exceeds the permitted use, you will need to obtain permission directly from the copyright holder. To view a copy of this licence, visit <http://creativecommons.org/licenses/by/4.0/>.

© The Author(s) 2021